

OPTICAL IMAGING OF METABOLISM IN HER2
OVEREXPRESSING CELLS

By

Alexandra Jule Walsh

Thesis
Submitted to the Faculty of the
School of Engineering of Vanderbilt University
in partial fulfillment of the requirements
for the degree of

MASTER OF SCIENCE
in
Biomedical Engineering

May, 2012

Nashville, Tennessee

Approved:

Professor Melissa C. Skala

Professor E. Duco Jansen

ACKNOWLEDGEMENTS

I would like to thank the funding sources that provided the equipment and supplies necessary for this project, including the Breast Cancer SPORE Developmental Project Award and Provost Graduate Fellowship. Experiments were performed in part through the use of the VUMC Cell Imaging Shared Resource (supported by NIH grants CA68485, DK20593, DK58404, HD15052, DK59637 and EY08126). Flow Cytometry experiments were performed in the VUMC Flow Cytometry Shared Resource. The VUMC Flow Cytometry Shared Resource is supported by the Vanderbilt Ingram Cancer Center (P30 CA68485) and the Vanderbilt Digestive Disease Research Center (DK058404).

Additionally, I would like to thank Professor Cook for her expertise on HER2 and for providing cells. Also, I would like to thank Dr. Arteaga and Dr. Rexer for development of the herceptin and lapatinib resistant cell lines. Many thanks to Madison Olive and Matthew Sundermann for help with cell culture.

ACKNOWLEDGMENTS.....	ii
LIST OF TABLES.....	v
LIST OF FIGURES.....	vi
CHAPTER	
1. INTRODUCTION.....	1
Overview of Breast Cancer.....	1
Introduction.....	1
Risk Factors.....	1
Diagnosis.....	4
Normal Breast Physiology.....	5
Common Breast Cancers.....	6
In Situ Carcinoma.....	6
Invasive Carcinoma.....	8
Role of Receptors.....	8
Estrogen Receptor (ER).....	8
Human Epidermal Growth Factor Receptor 2 (HER2).....	9
Current Treatments.....	10
Introduction.....	10
Targeted Breast Cancer Therapies.....	11
Resistance.....	13
Cellular Metabolism of Breast Cancer.....	14
Motivation.....	15
Fluorescence Imaging.....	15
Optical Imaging of Metabolism.....	16
Selection of Imaging Parameters.....	17
2. OPTICAL IMAGING OF METABOLISM IN HER2 OVEREXPRESSING BREAST CANCER CELLS.....	19
Introduction.....	19
Materials and Methods.....	22
Cell Culture.....	22
Verification of ER and HER2 Expression.....	24
Confocal Imaging.....	24
Image Analysis.....	25
Results.....	26
Verification of Optical Redox Ratio Measurement.....	27
Redox Ratio of HER2 Overexpressing Cells.....	28
Effect of HER2 Targeted Therapies.....	30
Discussion.....	31

3. CONCLUSIONS AND FUTURE WORK.....	35
Pre-clinical System Design.....	35
Clinical System Design.....	36
Future Directions.....	38
 REFERENCES.....	 39

LIST OF TABLES

Table	Page
1.1 Commonly used targeted therapies for breast cancer patients.....	12
2.1 Breast cancer cell lines with corresponding ER and HER2 expression.....	26
3.1 Design parameters for clinical optical metabolic monitoring system.....	37

LIST OF FIGURES

Figure	Page
1.1 Breast cancer incidence and mortality.....	3
1.2 Carcinoma in situ.....	7
1.3 Invasive carcinoma.....	7
1.4 HER2 and PI3K pathway.....	9
1.5 Jablonski diagram of fluorescence.....	16
1.6 Optical redox ratio.....	16
1.7 NADH and FAD fluorescence emission spectra.....	18
2.1 Expression of ER and HER2.....	26
2.2 Cyanide perturbation.....	27
2.3 Fluorescence and redox images.....	28
2.4 Redox ratio of malignant cells.....	28
2.5 Redox ratio normalized to proliferation rate.....	29
2.6 Effect of HER2 inhibitors on resistant and responsive cells.....	30

CHAPTER 1

INTRODUCTION

Overview of Breast Cancer

Introduction

According to the National Cancer Institute, 207,090 new cases of breast cancer are discovered each year (1). The incidence of breast cancer has increased by about 2% each year for the last few decades (2). While primary breast cancer tumors themselves are usually painless and have relatively few major complications, the tumors can metastasize and travel throughout the body, causing malignant tumors in essential organs which can result in death. The National Cancer Society estimates an average of 39,840 deaths from breast cancer annually (1). The probability of death from breast cancer varies widely across patients with differing tumor size, estrogen receptor status, and age of diagnosis (3). Breast cancer treatment and prognosis are greatly correlated with tumor expression of certain receptors, such as the estrogen receptor (ER) and the human epidermal growth factor receptor 2 (HER2).

Risk Factors

Breast cancer can occur in both genders; however, it is more prevalent in women than men (2). Genetic, hormonal, and dietary factors are thought to contribute to the

likelihood of the development of breast cancer (4). Numerous studies have investigated the effect of environmental factors versus genetic factors and the indications for development of breast cancer.

Breast cancer can be caused by genetic mutations. The high incidence of breast cancer among first degree relatives: grandmother, mother, aunt, daughter, or sister, suggests a strong genetic factor; however, families are likely to also live in similar environments and lifestyles (2). Five to ten percent of all women with breast cancer have a mutation of the BRCA-1 and BRCA-2 genes (5). Individuals with either but not both mutations do not have an increased incidence of breast cancer (5). The estimated lifetime risk of developing breast cancer for women with both mutations is estimated between 40-85% (5).

In addition to genetic predisposition, many environmental factors are correlated with an increased or decreased risk of breast cancer. Breast cancer has a much higher incidence in developed countries (2). Additionally, breast cancer occurs more frequently among women of professional or managerial professions as compared with manual labor workers (2). Obesity has also been linked to an increased risk of postmenopausal onset of breast cancer (2).

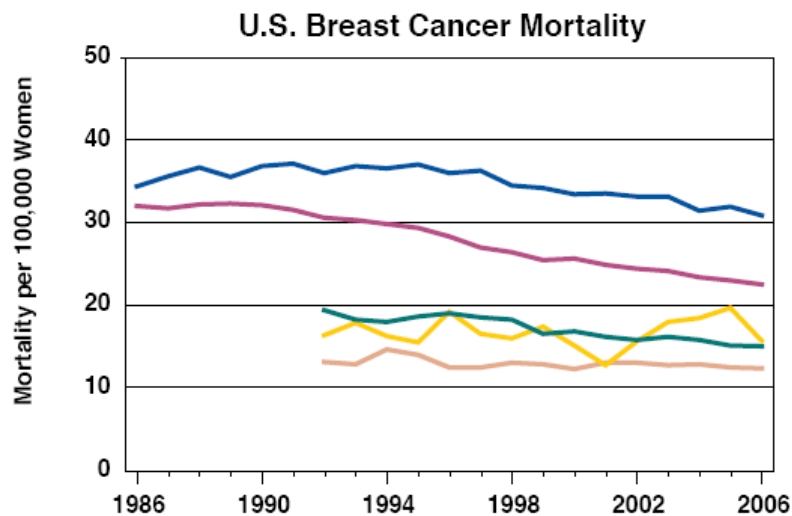
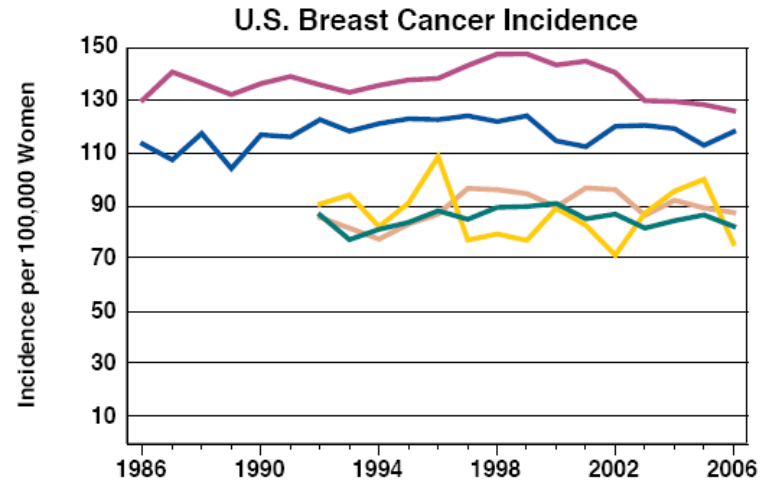


Figure 1.1: Breast cancer incidence and mortality. Incidence (1a) and mortality (1b) of American women with breast cancer across five ethnic groups: whites, Hispanics, African Americans, Asians/Pacific Islanders, and American Indians/Alaskan Natives (1).

Breast cancer incidence and mortality rates are linked with ethnicity (Fig. 1.1). According to reports from the National Cancer Institute, white American women have the highest incidence of breast cancer (6). However, African-American women have the highest mortality rates from breast cancer (6). Incidence and mortality of breast cancer is lowest in Hispanics, Asians/Pacific Islanders, and American Indians/Alaskan Natives.

Several risk factors have been correlated with higher risk for breast cancer development. Incidences of breast cancer increase with age (2). A prior history of benign breast disease is correlated with later onset of breast cancer (2). Also, radiation, from atomic bombs or medicinal purposes, such as tuberculosis treatments, is a direct cause of breast cancer (7). Many other factors have been investigated as indicators contributing to the development of breast cancer; however, often studies are inconclusive whether environmental factors are causal or incidental.

Diagnosis

The diagnostic process for breast cancer has evolved to include many procedures and imaging modalities. The initial suspicious lump is generally discovered by the patient or doctor during a physical examination (2). Symptoms of breast cancer include presence of a lump or thickening of the breast, change in the size or shape of the breast, changes in the skin of the breast, and fluid discharge (7). Usually the lump is painless, but on retrospect, the patient may remember mild discomfort from the area (2). Due to increased rates of survival and treatment outcomes with early cancer detection, women aged 50 to 74 are encouraged to have biennial screenings for breast cancer .

Several imaging modalities are used to detect lumps in the breast that are too small to be found in a physical exam. A mammogram is an x-ray image of the breast tissue which can show lumps and calcified tissues (7). Ultrasound can be used to image calcified tumors.(7). MRI images are also used to distinguish normal breast tissue from benign lesions (7).

Fine needle aspiration and core needle biopsy procedures extract cells of suspicious lumps for histological analysis. In fine-needle aspiration, a needle is used to extract a small amount of liquid from the cyst or lump to determine the pathology of the suspicious lesion (2). Fine-needle aspiration is performed on large tumors and fluid filled tumors. A core needle biopsy is used to extract cells of lesions that are less than 2 cm for histological analysis (2). Open surgical biopsy can also be performed if the lump is too small for the needle biopsies or if the needle biopsies are inconclusive (2).

Histopathology of the biopsied tissue provides characterization of the tumor and guides therapy selection. Pathologists inspect the cells for the presence of abnormal or cancerous cells. The biopsied cells are also stained for expression of ER and HER2 to determine if the patient is eligible for targeted therapies.

Normal Breast Anatomy

The normal breast consists of several structures including the fatty connective tissue, secretory lobes, and ducts. Breasts contain 15-25 lobes which are the tubulo-acinar glands (8). The lobes are arranged radially at different depths around the mammary papilla (8). Each lobe can be divided into lobules. A lobule is a system of ducts, the alveolar ducts (8).

Lobules are separated by loose connective tissue and lobes are separated by dense connective tissue and adipose tissue (8).

Common Breast Cancers

A carcinoma is a malignant tumor derived from epithelial cells (2). In breast tissue, epithelial cells line the ducts, acini, or lobules which are the locations where breast cancer can develop (2). When examined microscopically, cancer cells exhibit changes within the cell different from normal epithelial cells (2). When viewed macroscopically, the changes within the cells cause alterations in the arrangement of cells in relation to each other leading to the tumor appearance (2). Breast cancer can be divided into two main categories: in situ carcinoma and invasive carcinoma. In situ carcinoma is where the proliferating, malignant cells are confined by the basement membrane surrounding the ducts. Invasive carcinomas are cases where the proliferating cells invade the breast stroma and tissue spaces (2).

In Situ Carcinoma

In situ carcinoma is commonly expressed in association with invasive carcinoma; however, in situ carcinoma can present independently of invasive carcinoma in cases where the cancer cells are contained within the basal membrane of the duct (Fig. 1.2) (2). Between 1 and 5 % of breast cancer cases are independent in situ carcinoma, but this number is expected to increase as women are screened at increasingly younger ages (4). In situ carcinoma includes four classifications of breast cancer, ductal carcinoma, 59% of in situ carcinomas, lobular carcinoma, 28% of in situ carcinomas, Paget's disease, and intracystic

carcinoma (2). Often, mixed ductal and lobular carcinomas are observed in the same breast (1).

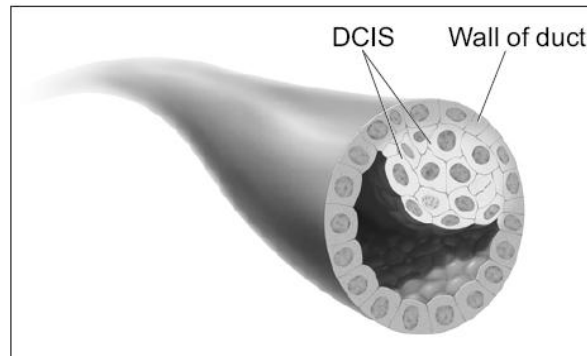


Figure 1.2: Carcinoma in situ. In ductal carcinoma in situ, diseased tumor cells are confined by the duct (7).

Histologically, ductal carcinoma tissue can appear normal or nodular with the involved ducts dilated, indurated, or containing a gray secretion (2). Ductal carcinoma can be found in any duct of the breast and often multiple ducts present with cancerous cells (7). The involved ducts are noticeably enlarged and may appear distorted but preserve a well-defined contour. As an in situ carcinoma, ductal carcinomas are surrounded by the basement membrane and confined to the ducts.

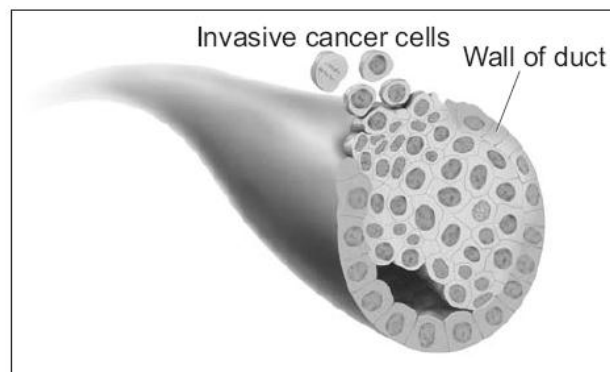


Figure 1.3: Invasive carcinoma. Invasive carcinoma cells outgrow the duct and spread into the surrounding tissue (7).

Invasive Carcinoma

When the cancer cells spread outside of the duct, the cancer is called invasive carcinoma (Fig. 1.3). The most common form of breast cancer is invasive ductal carcinoma which affects about 77% of all breast cancer cases (2). While these tumors have large variation in shape, size, and physiology; generally, invasive ductal carcinoma tumors include glandular structures and are separated by a fibrous membrane (4). Additional forms of invasive breast cancer include invasive lobular carcinoma, medullary carcinoma, mucinous carcinoma, among others; however, invasive carcinomas are more generally classified by stage to determine best treatment.

Role of Receptors

Estrogen Receptor (ER)

The estrogen receptor is not typically expressed in normal breast cells. The estrogen receptor is a transcription factor, meaning that upon activation by estrogen, the transcription of certain genes is increased (9). Estrogen receptors are found on the cells of many different organs including the endometrium and hypothalamus (10).

The estrogen receptor has several functions in breast cancer tumors. The estrogen receptor can act as a transcription factor. In this pathway, estrogen binds to the estrogen receptor causing it to phosphorylate, which dissociates several attached proteins such as heat shock protein 90 (HSP-90), resulting in an estrogen receptor with a different conformation

in an active form (11). The activated estrogen receptor binds with other factors, co-activators or co-repressors, in the nucleus to moderate gene transcription (11). Estrogen receptors can also activate non-genomic pathways in the cytoplasm. In one example, the activated estrogen receptor activates the mitogen-activated protein kinase pathway (MAPK) which increases cellular metabolism and promotes cell growth (11). Hormonal therapies, such as tamoxifen, bind ER without activating it, reducing the oncogenic effects of ER signaling.

Human Epidermal Growth Factor Receptor 2 (HER2)

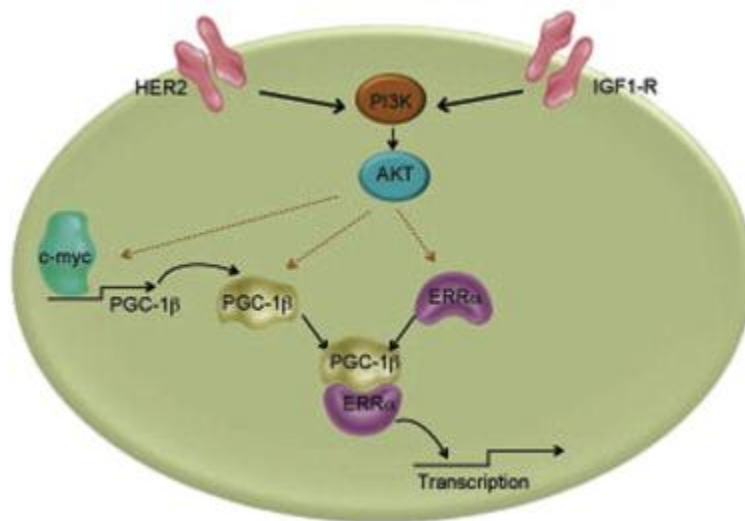


Figure 1.4: HER2 and PI3K pathway. HER2 pathway activation increases metabolism and glucose uptake through activation of PI3K and AKT (12).

HER2 is overexpressed in approximately 30% of primary breast cancer tumors and is associated with more aggressive tumors, increased recurrence, and poor patient outcomes (13). HER2 is commonly expressed in breast tissue, including non-cancerous cells; thus, overexpression beyond the basal expression of normal tissue is clinically monitored. Breast tumors are tested for HER2 overexpression by fluorescence in situ hybridization which

labels copies of the HER2 gene with fluorescence tags (14). The HER2 pathway is thought to activate PI3K, a major driver of cellular metabolism (Fig. 1.4). HER2 inhibitors prolong survival in responsive patients by impairing the oncogenic effects of HER2 signaling (15).

Current Treatments

Introduction

Core needle biopsy, fine-needle aspiration cytology, and histological confirmation are used to determine the malignancy of the tumor. A biopsy provides receptor status which guides treatment decisions (16). Mastectomy is a complete surgical removal of the infected breast. Common surgical management includes breast-conserving surgery paired with radiation therapy, mastectomy and reconstruction, and mastectomy without reconstruction. During surgery, lymph nodes are removed and dissected to determine whether metastases from the breast cancer tumors have migrated to the lymph nodes and throughout the body.

Treatments for breast cancer include surgical intervention, chemotherapy, radiation, and targeted therapeutics. Often, breast cancer treatment involves a multimodal approach, using several different therapies to combat different aspects of the disease. Age, menopausal state, disease stage, histology, and receptor expression influence the selection of therapy to optimize treatment to each specific cancer.

Doctors utilize a variety of treatments for ductal in situ carcinoma. Until recently, mastectomy was the most common surgical intervention and treatment of ductal in situ carcinoma (17). Mastectomy was preferred because other surgical interventions, such as partial removals, removing only the suspicious lesion, had a high recurrence, 25-50% while only 1-2% of mastectomy patients had recurrence; however lumpectomy, removal of the suspicious lesion plus a safety margin, procedures have greatly improved (17). Current

treatments for ductal in situ carcinoma involve a combination approach, attacking the cancer in several manners. The combined approach of tamoxifen therapy and surgery reduces same breast recurrence at 5 years and reduces contralateral occurrence (18, 19). The combined drug and surgery regimen seeks to remove the primary tumor and selectively kill remaining cancer cells.

Likewise, lobular in situ carcinoma is treated with a variety of treatment options. Lobular in situ carcinoma is not malignant but an indication that a woman is at increased risk for the development of invasive cancer (1). Tamoxifen is a common treatment for reducing the risk of developing breast cancer in women with lobular in situ carcinoma (20).

The treatment of late-stage or inflammatory breast cancer is a similar multimodal approach. A biopsy first provides histology of the breast cancer revealing ER status, progesterone receptor status, and HER2 status. Radiation, hormonal, and chemotherapy treatments are attempted initially (1). Upon favorable prognosis with the initial therapy, surgery will be performed (1). Stage IV, recurrent, and metastatic breast cancer is combated with a variety of surgical, radiation, and hormonal therapies. Traditionally, tamoxifen is used as a hormonal treatment for ER positive tumors.

Targeted Breast Cancer Therapies

Recent breast cancer research has focused on therapeutic agents targeting specific pathways within the cancerous cell. Breast cancers expressing the estrogen receptor (ER) are often treated with tamoxifen, an ER antagonist. Breast tumors which overexpress the human epidermal growth factor receptor 2 gene (HER2), which accounts for approximately 30% of all breast cancer patients, display more aggressive cancer

progression (13). Trastuzumab and lapatinib, two therapeutic agents that inhibit HER2, prolong survival in patients with HER2-overexpressing breast cancers (15, 21, 22).

Recent studies have proven that tamoxifen is an effective hormonal drug for the systemic treatment of breast cancer (22). An analysis of 80,273 women in 71 trials of tamoxifen found that after five years, the death rate by breast cancer was reduced by 31% (22). In this analysis, worse outcomes were associated with ER-negative receptor status and a longer duration of treatment (22). Current recommendations are that tamoxifen treatment be terminated after five years due to the development of tamoxifen resistant tumors (23, 24). Tamoxifen can be an advantageous anti-cancer agent for breast cancer cases of ER-positive tumors. Currently several estrogen receptor inhibitors are in clinical trials as possible alternatives to tamoxifen (1).

Breast cancers that overexpress HER2 are treated with HER2 inhibitors such as lapatinib and trastuzumab. A high concentration of HER2 receptors expressed by breast cancer cells is associated with increased tumor progression and metastases (14).

Trastuzumab is a monoclonal antibody that inhibits HER2 receptors. Additionally, the antibodies decrease the expression of HER2 in malignant cells which reduces tumor progression and metastases (14). Lapatinib is a small molecule inhibitor which binds HER2 and prevents the formation of activated HER2 dimers, preventing the activation of the HER2 cascade and reducing the oncogenic effects of HER2 signaling (21).

Drug	Receptor Target	Type
Tamoxifen	ER	Hormone
Lapatinib	HER2	Small molecule inhibitor
Trastuzumab (Herceptin)	HER2	Antibody

Table 1.1: Commonly used targeted therapies for breast cancer patients.

Due to the importance of choosing the correct treatment for breast cancer patients, tumors are screened for hormone receptors. Currently, malignancy, ER, and HER2 expression is determined by histology staining and fluorescence in situ hybridization (FISH). Both of these methods are time-consuming, relatively subjective, and costly due to the need for tissue slicing, processing and staining before expert evaluation. Development of a technology that could be used in the clinic to quickly and accurately quantify malignancy and receptor expression will enable earlier initiation of treatment, guide selection of effective treatment, and reduce health care costs.

Resistance

Another factor influencing treatment decisions and ultimately limiting the clinical outcome of breast cancers is resistance to targeted therapies. Only 57% of patients with ER-positive breast cancers respond to tamoxifen therapy (25). Similarly, approximately one-third of breast tumors that overexpress HER2 do not respond to trastuzumab and lapatinib therapy (26). However, novel therapeutics are in development to overcome clinical resistance to these therapeutic inhibitors (15). Early identification of the tumors that will respond to targeted therapies versus those that are resistant, will expedite clinical decisions regarding course of treatment, and will improve the clinical outcomes of breast cancer patients. Methods currently under development to determine tumor response to therapy include positron emission tomography (PET), CT and magnetic resonance imaging (MRI) (27-29). Evidence that tumor response to targeted inhibitors can be visualized was demonstrated with the use of fluoro-deoxyglucose (FDG)-PET, which is capable of detecting focused areas of high glucose uptake, such as is seen in many solid

tumors (30). A preliminary study of lapatinib-treated breast cancers showed changes in cellular metabolism, as measured by FDG-PET, after 1 month of lapatinib treatment (31). Yet, these currently available technologies provide only low resolution images, often require the use of radioactive contrast agents, and do not offer any information regarding HER2 or ER expression. Given the high cost of these procedures, it is unlikely that these will be adopted as standard of care, underscoring the need for more efficient, accurate, and cost-effective methods of identifying receptor expression and therapeutic response.

Cellular Metabolism of Breast Cancer

Cellular metabolism is a potentially powerful biomarker for tissue biopsy analysis. Unlike normal cells that rely on oxidative phosphorylation to generate ATP, or that use glycolysis under anaerobic conditions, cancer cells often generate ATP through aerobic glycolysis (32). This observation is generally described as the Warburg effect. Interestingly, ER and HER2 signaling in breast cancer cells drives aerobic glycolysis. ER increases glucose transport and glycolysis (33, 34). Similarly, HER2 activated pathways may increase glucose transport into the cell and increase glycolysis (35, 36). Furthermore, resistance to therapeutic agents, including the HER2 inhibitors lapatinib and trastuzumab, activates hypoxia signaling in the presence of adequate oxygen, consistent with the activation of aerobic glycolysis. Furthermore, PI3K pathway activation, which is a major driver of aerobic glycolysis, is often elevated in trastuzumab- or lapatinib-resistant breast cancer cells (37-40).

Motivation

A clinical need exists for a technology capable of predicting targeted therapy response by breast cancer cells and monitoring therapy effectiveness. This study tests the hypothesis that optical imaging of cellular metabolism can illuminate metabolic differences among cancerous cells and monitor therapy effectiveness and seeks to define the design parameters for a clinical device capable of monitoring therapy response. Optical imaging of metabolism may identify those cancer cells exhibiting the Warburg effect in response to ER and HER2 signaling. Metabolism imaging may identify those tumors exhibiting resistance to therapeutic inhibitors of these receptor pathways. Currently, FDG-PET is used to determine therapy response in vivo, yet is expensive, requires the injection of radioactive agents, and cannot be repeated frequently. Optical imaging has the potential to be developed as a tool to monitor cellular metabolism and therapy response.

Fluorescence Imaging

Particular molecules, called fluorophores, are capable of emitting a photon of longer wavelength when excited by a photon of an optimal energy. This phenomenon is illustrated in the Jablonski diagram (Fig. 1.5). Several biomolecules are natural fluorophores, including collagen, tryptophan, NADH, FAD, and elastin. These fluorophores are often referred to as 'auto-fluorescent' because the addition of fluorescent dyes or antibodies is not required.

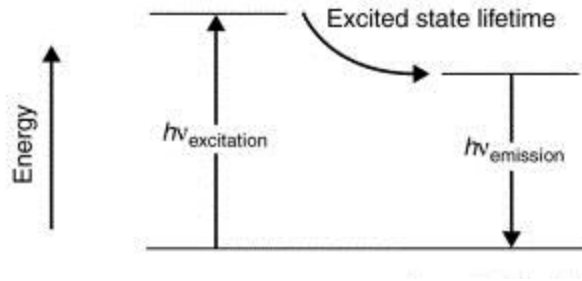


Figure 1.5: Jablonski diagram of fluorescence. When a fluorophore is excited by a photon ($h\nu_{\text{excitation}}$), the fluorophore enters an excited state. Sometime later, the fluorophore returns to ground state and emits a photon ($h\nu_{\text{emission}}$) (41).

Optical Imaging of Metabolism

Optical imaging is an ideal modality for probing chemical specificity and molecular contrast within tissues, including auto-fluorescence imaging of NADH and FAD, which allows quantitative measurements of cellular metabolism. In oxidative phosphorylation, NADH is oxidized to NAD^+ and FAD is reduced to FADH_2 (Fig. 1.6). In glycolysis, NAD^+ is reduced to NADH (Fig. 6). Because fluorescence intensity is proportional to fluorophore concentration, the optical redox ratio (NADH fluorescence intensity divided by FAD fluorescence intensity) represents relative amounts of glycolysis and oxidative phosphorylation within a cell (42).

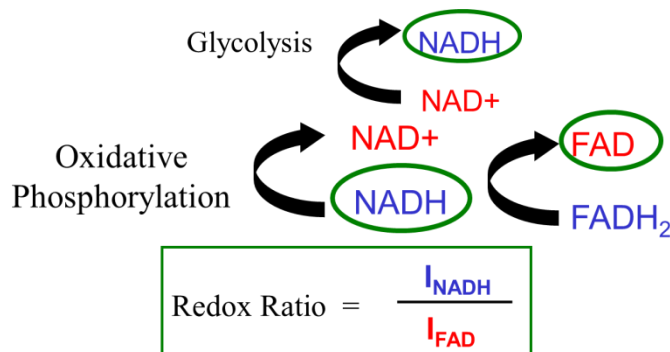


Figure 1.6: Optical redox ratio. The optical redox ratio is the relative intensity of cellular NADH fluorescence to FAD fluorescence.

The optical redox ratio is a proven method of probing cellular metabolism and has been used to differentiate cancerous from non-cancerous tissues in a variety of models including oral and breast cancer (42-48). Ostrander et al. showed the optical redox ratio is sensitive to ER expression in breast cancer cell cultures and that treatment with tamoxifen decreased the redox ratio of those cells that were responsive to tamoxifen, but not those that were resistant (48). The optical redox ratio is used in Chapter 2 to examine the changes in cellular metabolism due to HER2 expression and cellular response to HER2 targeted therapies.

Selection of Imaging Parameters

Particular excitation wavelengths and emission filters were chosen to ensure adequate isolation of NADH and FAD fluorescence. The peak excitation wavelength for NADH is near 350 nm and emission spans 400-500 nm (Fig. 1.7) (49). FAD excitation peak is near 450 nm. FAD emission spans 500-600 nm (Fig. 1.7) (49). For this study, NADH was excited at 405 nm, the lowest available excitation wavelength on the Olympus FV-1000 microscope. FAD was excited at 488 nm. Emission between 410-510 nm was collected for NADH, with the assumption that FAD excitation at 405 nm is negligible and FAD emission need not be filtered from the NADH emission. For FAD, 500-600 nm emission light was collected.

Isolation of NADH and FAD was verified by a cyanide experiment. Cyanide disrupts the electron transport chain preventing the conversion of NADH to NAD and FAD to FADH₂. Upon treatment with cyanide, an increase in NADH and a decrease in

FAD should be observed. The results of the cyanide experiment are presented in Chapter 2.

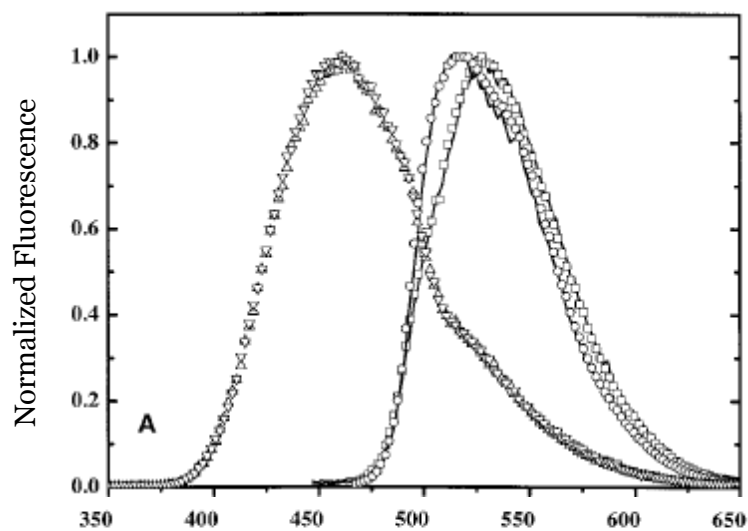


Figure 1.7. NADH and FAD fluorescence emission spectra. Fluorescence emission spectra for NADH (triangle) and FAD (circle) (49).

CHAPTER 2

OPTICAL IMAGING OF METABOLISM IN HER2 OVEREXPRESSING BREAST CANCER CELLS

Introduction

The course of breast cancer treatment increasingly relies on the molecular phenotype of the tumor. For example, breast cancers that overexpress the estrogen receptor (ER) are often treated with ER-antagonists such as tamoxifen, while those that overexpress human epidermal growth factor receptor 2 (HER2) are often treated with HER2-inhibitors (e.g., trastuzumab, lapatinib). HER2 overexpressing tumors display aggressive cancer progression (13) and account for approximately 30% of all breast cancer patients. Treatment with trastuzumab (a monoclonal antibody which binds HER2) and lapatinib (a dual tyrosine kinase inhibitor that binds both HER2 and the epidermal growth factor receptor) has been shown to prolong survival in patients with HER2 overexpressing breast cancers (21, 26, 50). Due to the importance of choosing the correct treatment for breast cancer patients, breast tumors are routinely screened for expression of ER and HER2. Currently, ER and HER2 expression are determined by immunohistochemistry (IHC) and fluorescence in situ hybridization (FISH).

Unfortunately, approximately one-third of breast tumors that overexpress HER2 do not respond to trastuzumab and lapatinib therapy (26). Similarly, only 57% of patients with ER-positive breast cancers respond to tamoxifen therapy (25). However, there are reasons to remain optimistic, as novel therapeutics are in development to overcome clinical resistance to these therapeutic inhibitors (15). Early identification of those

cancers that respond to targeted therapies versus those that are resistant will expedite clinical decisions regarding the course of treatment and will improve the clinical outcomes of breast cancer patients.

Methods currently under development to determine tumor response to therapy include positron emission tomography (PET), x-ray computed tomography (CT) and magnetic resonance imaging (MRI) (27-29). Evidence that tumor response to targeted inhibitors can be visualized was demonstrated with the use of fluoro-deoxyglucose (FDG)-PET, which is capable of detecting focused areas of high glucose uptake that are often seen in solid tumors. A preliminary clinical study of lapatinib-treated breast cancers showed changes in tumor metabolism after 1 month of lapatinib treatment (31). Yet, these currently available technologies provide only low resolution images, are non-portable, and usually require the use of radioactive contrast agents. Given the high cost of these procedures, it is unlikely that these will be adopted as standard of care, underscoring the need for more efficient, accurate, and cost-effective methods of identifying receptor expression and therapeutic response.

Cellular metabolism is a potentially powerful biomarker for tumor analysis. Unlike normal cells that rely on oxidative phosphorylation to generate ATP, or that use glycolysis under anaerobic conditions, cancer cells often generate ATP through aerobic glycolysis (32). Interestingly, signaling through the HER2 and ER pathways in breast cancer cells is thought to promote aerobic glycolysis. ER increases glucose transport and glycolysis (33, 34). Similarly, HER2 activated pathways may increase glucose transport into the cell and glycolysis (35, 36). HER2 signaling activates phosphatidylinositol 3-kinase (PI3K) a major driver of aerobic glycolysis (37-40). In mouse models of HER2

overexpressing breast cancer, trastuzumab and lapatinib inhibited PI3K activity and decreased glucose uptake as measured by FDG-PET imaging (51). Conversely, breast tumor cells exhibiting resistance to HER2 inhibitors display aberrantly increased PI3K activity and active hypoxia signaling despite the presence of adequate oxygen (39). These studies suggest that differences in aerobic glycolysis may reflect not only oncogene-driven metabolic characteristics of the tumor cell, but also the effect of therapeutic inhibitors on tumor metabolism, and could therefore be used to distinguish tumors that are responsive to therapeutic inhibitors from those that are resistant.

During oxidative phosphorylation, NADH is oxidized to NAD⁺ and FAD is reduced to FADH₂. However, the process of glycolysis causes NAD⁺ to be reduced to NADH. Therefore, the ratio of NADH to FAD is a measurement of the balance between glycolysis (seen in tumor cells) and oxidative phosphorylation (seen in untransformed cells). NADH and FAD can be measured *in situ* using autofluorescence optical imaging techniques. The optical redox ratio (NADH fluorescence intensity divided by FAD fluorescence intensity) is a proven method of probing cellular metabolism and has been used to differentiate cancerous from non-cancerous tissues in a variety of models including oral and breast cancer (42-48). Ostrander et al. showed the optical redox ratio is also sensitive to ER expression in breast cancer cell cultures, and that treatment with tamoxifen decreased the optical redox ratio of tamoxifen-sensitive cells, but not tamoxifen-resistant cells (48).

The purpose of this study was to determine the effect of HER2 overexpression on the metabolism of breast cancer cells as measured by the optical redox ratio to determine if optical redox monitoring can be used as a simple, effective, low-cost biomarker for

monitoring HER2 status. The hypothesis that HER2 overexpression influences cellular redox ratios independently of ER expression was tested. Additionally, the impact of HER2 inhibition on the redox ratio in HER2 overexpressing breast cancer cells was measured. Finally, we determined if therapeutic resistance to HER2 inhibitors reflected on redox ratio measurements as a failure to reduce redox ratios in response to HER2 inhibition. HER2 overexpression was found to increase the redox ratio, independently of ER expression. While HER2 inhibition decreased the optical redox ratios in HER2 overexpressing cells, the HER2 inhibitor, trastuzumab, had no impact on redox ratios in trastuzumab resistant cells, despite continued overexpression of HER2.

Materials and methods

Cell Culture

MCF10A cells were cultured in Mammary Epithelial Cell Growth Medium (MEGM, Lonza, Walkersville, MD) excluding the gentamycin-amphotericin B mix and supplemented with 100 ng/ml cholera toxin and 1% penicillin:streptomycin. The BT474, MDA-MB-231, MCF7, and SKBr3 cells were grown in DMEM (Invitrogen, Carlsbad, CA), supplemented with 10% fetal bovine serum and 1% penicillin:streptomycin, hereafter referred to as DMEM+. The resistant cell lines were grown in the DMEM+ at levels of the corresponding drug to maintain resistance. The lapatinib resistant cells were grown at 1 μ M lapatinib (LC Laboratories, Woburn, MA) concentration and the trastuzumab resistant cells were grown at 25 μ g/ml.

For imaging, all cell lines were plated at a density of 1×10^5 cells per 35 mm plate, 48 hours prior to imaging. Glass bottom dishes (MatTek Corporation, Ashland, MA)

were used to allow live cell imaging on an inverted, confocal microscope. The trastuzumab and lapatinib resistant cell redox ratio was determined from cells grown in trastuzumab and lapatinib supplemented media. For the drug perturbation experiments, the responsive BT474 cells were fed the drug supplemented media 24 hours prior to imaging. For the trastuzumab perturbation of the trastuzumab resistant cells, the cells were fed the DMEM+ media for the first 24 hours after plating and the DMEM+ with trastuzumab for the second 24 hours. Drug concentrations of the media were selected to mimic therapeutic drug dosage in patients, 25 $\mu\text{g/ml}$ for trastuzumab (VUMC Pharmacy, Nashville, TN) and 2 μM for tamoxifen (Sigma-Aldrich, St. Louis, MO) (51, 52).

In order to verify isolation of NADH and FAD auto-fluorescence, a cyanide experiment was conducted. MCF10A cells were plated at 1×10^5 cells per plate, 48 hours prior to imaging. Cells were imaged before the addition of cyanide. After 3 images from a plate were acquired, the cell media was exchanged for growth media supplemented with 4 mM NaCN (Sigma-Aldrich, St. Louis, MO). The cells were given one minute to react with the cyanide; then, 3 different places of each plate were imaged.

Proliferation rates of MCF10A, MCF7, and BT474 cells were determined by antibody labeling of cells grown on parallel imaging plates. Mitotic cells were first marked using a Phospho-Histone H3 (Ser10) antibody (Cell Signaling Technology, Danvers, MA). Then, labeling of the primary antibody with Alexa Fluor 488 goat anti-rabbit IgG antibody (Invitrogen, Carlsbad, CA) allowed counting by flow cytometry of the highly fluorescent mitotic cells and the less-fluorescent unlabeled cells. The percentage of proliferating cells was determined by dividing the number of highly fluorescent cells into the total number of cells counted.

Verification of ER and HER2 Expression

Cells were homogenized in ice-cold lysis buffer [50 mM Tris pH 7.4, 100 mM NaF, 120 mM NaCl, 0.5% NP-40, 100 μ M Na₃VO₄, 1X protease inhibitor cocktail (Roche)], sonicated for 10 s at 4°C, 13,000 x g for 5 min. Protein concentration was determined using the BCA assay (Pierce). Proteins were separated by SDS-PAGE and transferred to nitrocellulose membranes. Membranes were blocked in 3% gelatin in TBS-T [Tris-buffered saline, 0.1% Tween-20) for 1 h, incubated in primary antibody in 3% gelatin for 2 h at room temperature, washed with TBS-T, incubated in HRP-conjugated anti-rabbit or anti-mouse IgG, washed with TBS-T, and then developed using ECL substrate (Pierce). The following primary antibodies were used: ErbB2 (HER2) (Neomarkers, InVitrogen; 1:2000); ER-alpha (Santa Cruz Biotechnologies; 1:1000); beta actin (Sigma-Aldrich; 1:5000).

Confocal Imaging

Images were acquired using an Olympus FV-1000 Inverted Confocal Microscope with a 40X/1.3 NA oil-immersion objective. Confocal microscopy was chosen over widefield fluorescence to reduce background noise for ease of NADH and FAD autofluorescence measurement. Additionally, the redox ratio is sensitive to measurement volumes and confocal microscopy ensures that the NADH and FAD signals can be co-registered to the same volume. For NADH fluorescence, the cells were excited at 405 nm and 410-510 nm emission was collected. FAD was excited at 488 nm and 500-600 nm emission was collected. The two images were acquired simultaneously, with NADH and

FAD acquired sequentially for each pixel. A pixel dwell time of 2 μ s was used. Each line was averaged 4 times to reduce noise. A single 1024x1024 pixel image required 39.0 s to acquire. To ensure the cells were not photobleaching, two images of the same field of view were acquired consecutively with no significant change in average pixel intensity. Settings for the gain, offset, and pinhole were maintained constant across all imaging sessions. To account for daily variations in laser power or instrumentation instability, the images were normalized to MCF10A cell measurements acquired during each imaging session. Each plate was imaged at 3 different, non-overlapping locations.

Image Analysis

The optical redox ratio, NADH fluorescence intensity divided by FAD fluorescence intensity, was computed for each cell in the image using ImageJ software (NIH). The fluorescence signal of non-cellular regions, or background signal, was removed to ensure the fluorescence comparisons were made only for the cells. NADH and FAD used for cellular metabolism are contained within the cytoplasm and mitochondria, and the fluorescence signal from the nucleus is not involved in cellular metabolism. Therefore, the fluorescence signal from the nucleus was also removed to ensure isolation of metabolic NADH and FAD and eliminate the possibility of nuclear size as a confounding factor. Next, a NADH/FAD per pixel image was computed and the redox ratio for each cell in the image was determined. The average redox ratio value from all cells in each image was computed and normalized to the corresponding session's MCF10A measurement. Standard error was computed from the mean redox ratio value across all images from each cell line. A rank sum test was used for all statistical comparisons.

Results

The optical redox ratio of a panel of human breast-derived cell lines with varying expression of ER and HER2 were studied (Table 2.1, Fig. 1.1). MCF10A, a non-cancerous breast cell line with negligible or low expression of ER and HER2 was used as a control for each analysis. Western blot analysis verified the expression of ER and HER2 (Fig. 1.1).

Cell line	Cancerous	ER status	HER2 overexpression	n
MCF-10A	Non-cancerous	- / low	- / low	30
MDA-MB-231	Cancer	Negative	Negative	15
MCF-7	Cancer	Positive	Negative	15
BT-474	Cancer	Positive	Positive	15
SKBr3	Cancer	Negative	Positive	15
HR6 (Trastuzumab Resistant BT-474)	Cancer	Positive	Positive	15
BT-LR (Lapatinib Resistant BT-474)	Cancer	Positive	Positive	15

Table 2.1: Breast cancer cell lines with corresponding ER and HER2 expression.

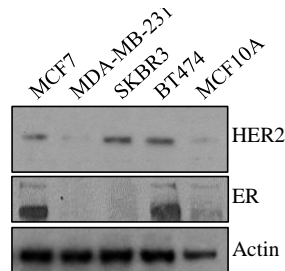


Figure 2.1: Expression of ER and HER2. Western blot analysis demonstrates overexpression of HER2 in the SKBR3 and BT474 cells and expression of ER in the MCF7 and BT474 cells.

Verification of Optical Redox Ratio Measurement

To verify the use of optical imaging to measure the redox ratio, cyanide was used to disrupt the electron transport chain, thus preventing the conversion of NADH to NAD⁺ (53). As predicted, MCF10A cells treated with cyanide exhibited increased NADH fluorescence ($p < 0.01$, Fig. 2.2) and decreased FAD fluorescence ($p < 0.05$; Fig. 2.2). Therefore, the redox ratio was increased in cyanide-treated MCF10A cells as compared to untreated cells ($p < 0.005$, Fig. 2.2). These results confirm that our optical imaging methods accurately reflect the balance between glycolysis and oxidative phosphorylation, and can be used to assess the metabolic state of tumor cells.

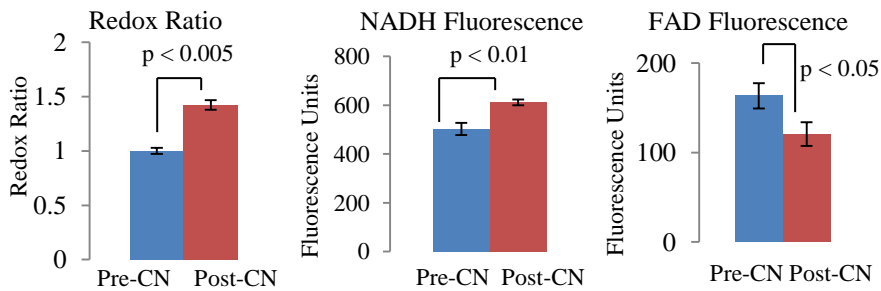


Figure 2.2. Cyanide perturbation. Addition of CN to MCF10A cells ($n = 6$) results in an increase in redox ratio and NADH fluorescence and a decrease in FAD fluorescence. Bar height represents mean and error bars represent SE.

Redox Ratio of HER2 Overexpressing Cells

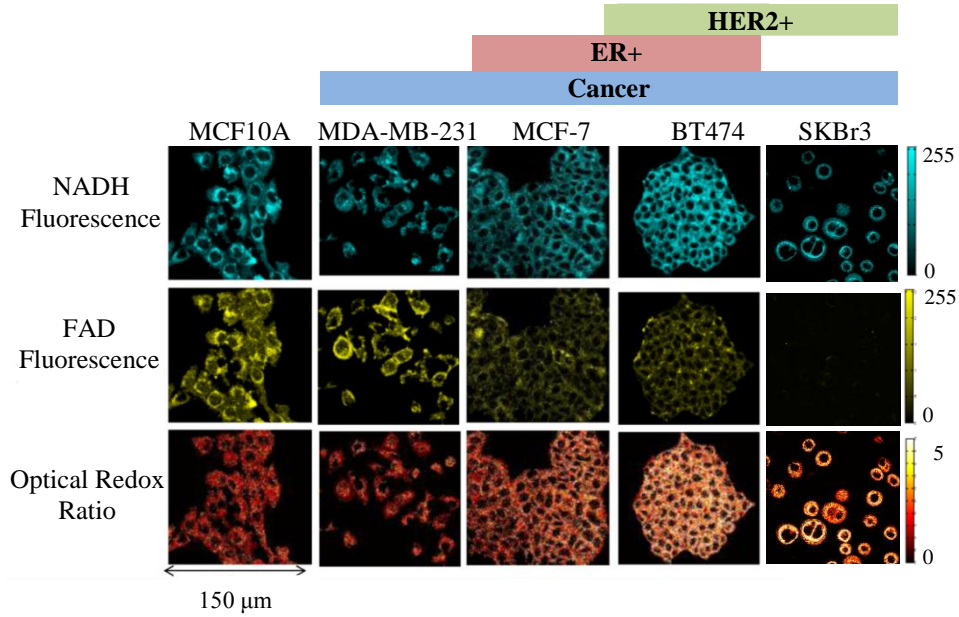


Figure 2.3. Fluorescence and redox images. Representative NADH, FAD, and redox ratio images for MCF10A, MDA-231, MCF7, BT474 and SKBr3 cells. Optical redox ratio increases with ER and HER2 expression.

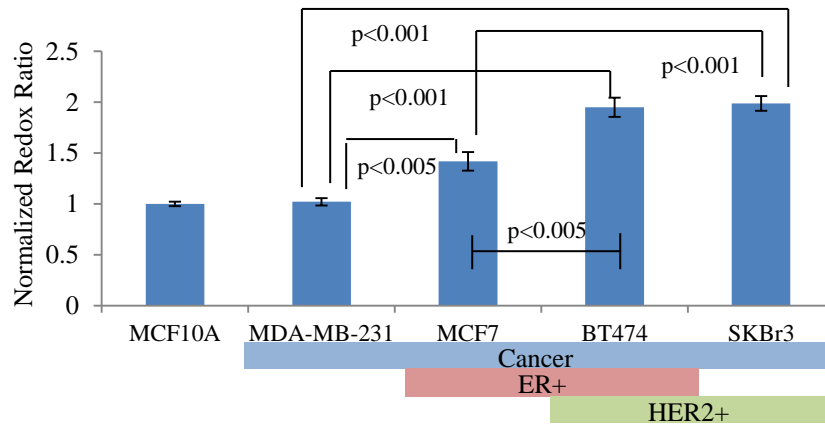


Figure 2.4. Redox ratio of malignant cells. Quantitative representation (mean +/- SE) of the redox ratio values for the MCF10A (n=30), MDA-MB-231 (n=15), MCF7 (n=15), BT474 (n=15), and SKBr3 cells (n=15). Redox ratio is elevated in cells overexpressing HER2.

We used optical imaging to capture NADH and FAD fluorescence in five breast derived cell lines (Fig. 2.3): MCF10A (untransformed breast epithelial cells), MDA-MB-231 (ER-/HER2-), MCF-7 (ER+/HER2-), SKBR3 (ER-/HER2+), and BT474 (ER+/HER2+). The fluorescence intensities were used to calculate the redox ratio per cell for each cell line (Fig. 2.4). While ER-/HER2- MDA-MB-231 cells displayed a redox ratio that was similar to what was seen in untransformed MCF10A cells, redox ratios were elevated in all other breast cancer cell lines ($p < 0.005$). ER+/HER2- breast cancer cell lines displayed elevated redox ratios ($p < 0.005$), but not to the extent seen in HER2+ breast cancer cell lines ($p < 0.001$).

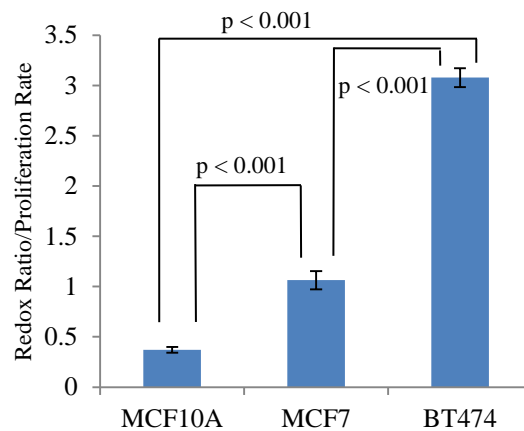


Figure 2.5. Redox ratio normalized to proliferation rate. Redox ratio divided by proliferation rate mean \pm SE for MCF10A (n=30), MCF7 (n = 15) and BT474 (n = 15) cells.

Controlling for differences in rates of proliferation among the MCF10A, MCF7, and BT474 cells did not reduce the significance of the redox ratio results shown in Fig. 2.4. In fact, controlling for proliferation (redox ratio divided by proliferation rate for each cell line) increases the differences between these three cell lines (Fig. 2.5).

Effect of HER2 Targeted Therapies

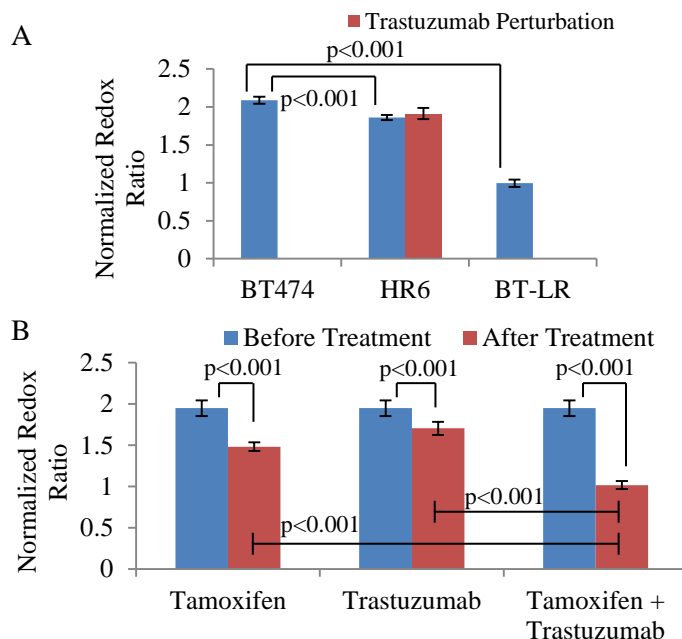


Figure 2.6. Effect of HER2 inhibitors on resistant and responsive cells. (A) The redox ratio (mean \pm SE) of responsive BT474 cells is different from the trastuzumab (HR6) and lapatinib (BT-LR) resistant cells ($n=15$), and there was no change in the redox ratio of trastuzumab-resistant HR6 cells with trastuzumab-treatment. (B) The redox ratio of responsive BT474 cells decreased with tamoxifen ($2 \mu\text{M}$), trastuzumab ($25 \mu\text{g/ml}$), and tamoxifen + trastuzumab treatment ($n=15$).

The redox ratio of both the trastuzumab resistant cell line, HR6, and the lapatinib resistant cell line, BT-LR, was lower than the redox ratio for the responsive parental BT474 cells (Fig. 2.6A). The HR6 cells are BT474-derived cells that continue to grow in the presence of trastuzumab (54). Likewise, the BT-LR cells are BT474-derived cells that were selected in culture with increasing concentrations of lapatinib (55). To investigate the contributions of the ER and HER2 signaling pathways to the redox ratio, BT474 cells (ER+/HER2+) were exposed to the ER antagonist tamoxifen and the anti-HER2 monoclonal antibody trastuzumab, (Fig. 2.6B). Trastuzumab significantly decreased the redox ratio in ER+/HER2+ breast cancer cells ($p < 0.001$; Fig. 2.6B).

Similarly, tamoxifen resulted in a decrease in redox ratio in the same cells ($p < 0.001$, Fig. 2.6B). The combination of tamoxifen with trastuzumab decreased the redox ratio in BT474 cells (ER+/HER2+) to a greater extent than single agent tamoxifen ($p < 0.001$) or trastuzumab ($p < 0.001$; Fig. 2.6B). Interestingly, treatment of HR6 cells with trastuzumab did not cause any alterations in the redox ratio (Fig. 2.6A). It is difficult to fully eliminate the influence of lapatinib on the BT-LR cells; and therefore, outside the scope of this study to robustly perform a comparison of pre- and post- lapatinib treatment in these cells.

Discussion

The selective use of aerobic glycolysis over oxidative phosphorylation by cancer cells has been known for over a century. We and others have shown that this characteristic of cancer cells can be monitored *in situ* using optical imaging to measure the redox ratio, or the ratio of glycolysis to oxidative metabolism. Furthermore, we show that “driver” oncogenes in breast cancer cells also drive aerobic glycolysis in these cells. Specifically, HER2 activity was required for maximal aerobic glycolysis in breast cells overexpressing HER2, while ER signaling was required for aerobic glycolysis in ER+ breast cancer cells. These results demonstrate the effect of the HER2 and ER signaling pathways on cancer cell metabolism, as measured by the optical redox ratio. These data support the conclusion that optical imaging of redox ratios can be used to measure the tumor cell response to therapeutic inhibitors *in situ*. Finally, using HER2 overexpressing breast cancer cells with acquired resistance to HER2 inhibitors, we demonstrated that loss of oncogene dependence was reflected in the optical redox ratio measurement, such that

HER2 inhibitors failed to decrease the redox ratio in a resistant cell line. Therefore, these findings could be applied to future studies using optical imaging of breast cells and tumors to predict their response to HER2 inhibitors, a development that would significantly inform clinical decisions regarding therapeutic strategies used to treat patients with HER2-positive breast cancers.

While this is the first study to correlate HER2 overexpression and activity to the redox ratio, a previous study similarly determined that ER+ breast cells exhibited a higher optical redox ratio than ER-negative cells (48). The previous study differs from the results presented herein because the previous study suggested that MCF7 cells (ER+/HER2-) exhibited a similar redox ratio to BT474 cells (ER+/HER2+). However, our results suggest that BT474 cells have significantly higher redox ratios than MCF7 cells. Several experimental factors could explain the differing results, including different excitation wavelengths for NADH, differing emission filters, and different growth media. Ostrander et al. used media supplemented with 5% FBS versus 10% used in our studies, which may have increased cellular proliferation in our experiments versus those described earlier, thus affecting tumor cell metabolism (56). However, when controlling for cell proliferation, the difference in the redox ratio between MCF7 and BT474 cells increased in the current study (Fig. 2.5). Different emission filters capture different areas of the NADH and FAD emission curves, affecting absolute fluorescence intensity which may change the redox ratio. The results of the cyanide experiment ensure measurement of NADH and FAD fluorescence for this study (Fig 9).

The results show that redox ratios in triple-negative MDA-MB-231 cells were similar to what was seen in MCF10A cells, which was less than the redox ratio seen in

HER2+ or ER+ breast cancer cells. Triple-negative breast cancers (TNBC) lack HER2, ER, and PR, so they are difficult to target and no molecular targeted therapies exist for these breast cancers. Several FDG-PET studies in TNBC, ER+, and HER2+ tumors report high variability in the glucose uptake of triple negative cells (57, 58). Note that FDG-PET imaging illuminates different aspects of cellular metabolism (glucose uptake) than the optical redox ratio (relative concentrations of NADH and FAD, end products of metabolism). However, these previous reports indicate that the metabolism of TNBC is complex and heterogeneous, so a full characterization of this tumor subtype will likely require a more concentrated study.

The highest redox ratios were measured in breast cancer cell lines with HER2 overexpression. The higher redox ratio of HER2 overexpressing cells suggests that the HER2 pathway may affect cellular metabolism. Indeed, studies have found increased concentrations of glucose transporters and glycolytic enzymes present in HER2 overexpressing cells versus cells with low expression of HER2 (35, 36).

We found that HER2 inhibition with trastuzumab decreased the redox ratio of HER2 overexpressing breast cancer cells ($p < 0.001$, Fig. 2.6B). This is consistent with several studies reporting reduced glucose uptake, decreased lactate secretion, and decreased glycolysis, in responsive HER2 overexpressing breast cancer cells treated with trastuzumab (59, 60). Treatment with both trastuzumab and tamoxifen decreased the redox ratio of responsive BT474 cells to levels seen in the non-cancerous MCF10A cell line (Fig. 2.6B). These results suggest that both ER and HER2 signaling affects tumor cell metabolism in breast cancer cells. Mechanistic studies of receptor expression support this result. Cells expressing ER overexpress glucose transporters and have higher

reported rates of glycolysis (33, 34). Similarly, HER2 overexpression is linked with increased glucose transport into cells and increased glycolysis (35, 36).

Innate and acquired resistance to HER2 inhibitors limits their current clinical success. Nearly all HER2-amplified breast cancers treated with trastuzumab or lapatinib will ultimately develop resistance to these targeted inhibitors. We examined trastuzumab-resistant cells, demonstrating that trastuzumab failed to reduce the redox ratio in the resistant cells (Fig. 2.6A). These results are the first of its kind, but are consistent with an FDG-PET study of trastuzumab responsive and non-responsive breast cancer xenographs, demonstrating that HER2 inhibitors failed to reduce FDG uptake in those tumors whose growth was unaffected by trastuzumab (61). Interestingly, the redox ratio of the trastuzumab and lapatinib resistant cells are different from the pre-treatment redox ratio value of responsive BT474 cells, $p < 0.001$ (Fig. 2.6A). These results open up the possibility of screening HER2-inhibitor resistance with the optical redox ratio.

Future *in vivo* studies are needed to verify the influence of ER and HER2 expression on cellular metabolism. Increasing research is elucidating the importance of metabolism in cancer cells and its relationship with drug resistance. Here, upon treatment with receptor targeted therapies, the change in metabolism of resistant cells is shown to be negligible, while the metabolism of responsive cells is significant. Additionally, basal redox ratios are different in resistant versus responsive cells. Therefore, cellular redox ratios may prove an invaluable tool for research and clinical identification of receptor expression, tumor resistance to targeted therapies, and for monitoring treatment efficacy.

CHAPTER 3

CONCLUSION AND FUTURE DIRECTIONS

Increased optical redox ratios were found in breast cancer cells overexpressing HER2. Upon treatment of responsive cells with HER2 targeted therapies, the redox ratio was reduced, supporting research that has correlated HER2 overexpression with increased glycolysis. Cells overexpressing HER2 but resistant to HER2 targeted therapies expressed reduced optical redox ratios compared to HER2-therapy responsive cells. These results suggest that the optical redox ratio may be further developed as a tool for predicting response to therapy and monitoring therapy effect on cellular metabolism.

Pre-clinical System Design

The optical redox ratio results presented in Chapter 2 indicate that a pre-clinical device may be developed to monitor therapy response in pre-clinical drug studies. Currently, to monitor drug efficacy in pre-clinical models such as mice xenograft tumors, the mice are sacrificed at certain hours post-treatment for histological and immunohistochemical analysis of the tumor response. Optical redox imaging may be used non-invasively through the mouse skin or an implanted window chamber to image the tumor's metabolic response non-invasively. Currently PET is utilized in such a manner; however, PET shows no difference between responders and non-responders until seven days post-treatment (30). Additionally, PET measurements require lengthy

recovery times due to the high radiation exposure and the time for the dye to wash through the mouse. Optical techniques are not limited by radiation or dyes and thus can be used at any time of interest.

A pre-clinical system design would require a fluorescence microscope capable of isolating NADH and FAD fluorescence emission. NADH can be excited around 350 nm and FAD around 480 nm. Emission filters can isolate NADH emission, 400-500 nm, and FAD emission 500-600 nm. For pre-clinical mouse studies, the device can image tumors through window chambers which allow utilization of a normal microscope. As the results presented in Chapter 2 show, such a device would need to be sensitive to optical redox ratio changes of at least 30% to effectively monitor metabolism.

A sub-cellular resolution is required of a pre-clinical system. Sub-cellular resolution allows isolation of different sub-populations of tumor cells with different responses to therapy. Several current microscopic techniques, such as confocal microscopy and two-photon fluorescence imaging allow sub-cellular resolution and could be implemented in the pre-clinical system.

Clinical System Design

In addition to development as a pre-clinical tool, the optical redox ratio has the potential to be developed as a simple, effective, low cost method for identifying HER2 overexpressing tissue and monitoring therapy in patients. Based on the results presented in Chapter 2, such a device may be capable of identifying HER2 overexpressing tumors,

predicting drug response, and with repeated measurements over time, monitoring therapy response. Table 3.1 illustrates several of the design parameters for such a device.

Feature	Design Constraints	Justification
Excite NADH	~ 350 nm	Measure NADH auto-fluorescence
Excite FAD	~ 480 nm	Measure FAD auto-fluorescence
Isolate NADH from FAD emission	~ 400-500 nm / ~500-600 nm	Need isolation of NADH and FAD fluorescence
Resolution	Cellular	Sub-populations of cells may respond differently
Depth	Best possible	Sampling core and inner tumor may have different redox states
Sensitivity	Must measure ~30% difference	This is the difference observed in the ER+/HER2- cells
Size	Fit into core needle	Clinical measurements

Table 3.1 Design parameters for clinical optical metabolic monitoring system.

A clinical system would need to be capable of exciting and isolating NADH and FAD auto-fluorescence. Excitation for NADH can be achieved around 350 nm and around 480 nm for FAD. Filters can be used to isolate the two emission signals, with NADH emission between 400 and 500 nm and FAD between 500 and 600 nm. Cellular resolution may be required as tumors are thought to be composed of sub-populations of cells with different gene expression which enables some cells to develop resistance to therapeutic agents (15). The device must be able to measure changes in redox ratio of at least 30%, as that is the difference between normal and ER+/HER2+ cells found in Chapter 2. Additional filters to block excitation light and room light from reaching the detector will help increase device sensitivity.

A large device, such as incorporation of fluorescence components into a surgical microscope, would require invasive procedures such as surgery to expose the tumor. Repeated measurements over time would not be possible from a surgical microscope. A clinical device would be most utilized if it may fit within a core needle to obtain measurements before core needle biopsy procedures. A micro-imaging system would allow multiple measurements during minimally invasive procedures. This design would also allow measurements at the time of diagnosis, during surgery, and post-surgery to monitor therapy response.

Several different fluorescence microscope designs can be used to isolate z-depth information from tissue including confocal microscopy, two-photon fluorescence microscopy, and wide-field fluorescence with structured illumination. A wide-field fluorescence microscope using structured illumination for depth resolution can be implemented to isolate the z-direction without the need for a confocal design. Wide-field microscopes are advantageous due to image acquisition speed.

Future Directions

Further studies are necessary for the development of the optical redox ratio for clinical use. Measurements from breast tumors are required to verify that the redox ratio remains sensitive to metabolic changes within a diverse patient population. These studies will further define the parameters of a clinical system. Furthermore, other optical techniques, such as the fluorescence lifetime of NADH and FAD, may provide important metabolic information and should be investigated.

REFERENCES

1. Breast Cancer Treatment: US Institutes of Health.
2. Hoogstraten J, George W, Bloom H. *Breast Cancer*. Berlin: Springer-Verlag; 1989.
3. Schairer C, Mink PJ, Carroll L, Devesa SS. Probabilities of death from breast cancer and other causes among female breast cancer patients. *J Natl Cancer Inst*. 2004;96(17):1311-21.
4. Dickson R, Lippman ME, McGuire W. *Breast Cancer: Cellular and Molecular Biology*. Boston: Kluwer Academic Publishers; 1988.
5. Blackwood MA, Weber BL. BRCA1 and BRCA2: from molecular genetics to clinical medicine. *J Clin Oncol*. 1998;16(5):1969-77.
6. Incidence and Mortality Rate Trends: National Cancer Institute.
7. Breast Cancer: National Institutes of Health; 2009.
8. Wheater PR, Burkitt HG, Daniels VG. *Functional Histology*. 2 ed. New York: Churchill Livingstone; 1987.
9. Levin ER. Integration of the extranuclear and nuclear actions of estrogen. *Mol Endocrinol*. 2005;19(8):1951-9. PMID: 1249516.
10. Yaghmaie F, Saeed O, Garan SA, Freitag W, Timiras PS, Sternberg H. Caloric restriction reduces cell loss and maintains estrogen receptor-alpha immunoreactivity in the pre-optic hypothalamus of female B6D2F1 mice. *Neuro Endocrinol Lett*. 2005;26(3):197-203.
11. Eroles P, Bosch A, Bermejo B, Lluch A. Mechanisms of resistance to hormonal treatment in breast cancer. *Clin Transl Oncol*. 2010;12(4):246-52.
12. Chang CY, Kazmin D, Jasper JS, Kunder R, Zuercher WJ, McDonnell DP. The metabolic regulator ERRalpha, a downstream target of HER2/IGF-1R, as a therapeutic target in breast cancer. *Cancer Cell*. 2011;20(4):500-10. PMID: 3199323.
13. Ross JS, Fletcher JA. The HER-2/neu oncogene in breast cancer: prognostic factor, predictive factor, and target for therapy. *Stem Cells*. 1998;16(6):413-28.
14. Freudenberg JA, Wang Q, Katsumata M, Drebin J, Nagatomo I, Greene MI. The role of HER2 in early breast cancer metastasis and the origins of resistance to HER2-targeted therapies. *Exp Mol Pathol*. 2009;87(1):1-11. PMID: 2735009.

15. Esteva FJ, Yu DH, Hung MC, Hortobagyi GN. Molecular predictors of response to trastuzumab and lapatinib in breast cancer. *Nat Rev Clin Oncol.* 2010;7(2):98-107.
16. Fisher B, Fisher ER, Redmond C, Brown A. Tumor nuclear grade, estrogen receptor, and progesterone receptor: their value alone or in combination as indicators of outcome following adjuvant therapy for breast cancer. *Breast Cancer Res Treat.* 1986;7(3):147-60.
17. Fonseca R, Hartmann LC, Petersen IA, Donohue JH, Crotty TB, Gisvold JJ. Ductal carcinoma in situ of the breast. *Ann Intern Med.* 1997;127(11):1013-22.
18. Fisher B, Dignam J, Wolmark N, Wickerham DL, Fisher ER, Mamounas E, et al. Tamoxifen in treatment of intraductal breast cancer: National Surgical Adjuvant Breast and Bowel Project B-24 randomised controlled trial. *Lancet.* 1999;353(9169):1993-2000.
19. Houghton J, George WD, Cuzick J, Duggan C, Fentiman IS, Spittle M. Radiotherapy and tamoxifen in women with completely excised ductal carcinoma in situ of the breast in the UK, Australia, and New Zealand: randomised controlled trial. *Lancet.* 2003;362(9378):95-102.
20. Fisher B, Costantino JP, Wickerham DL, Redmond CK, Kavanah M, Cronin WM, et al. Tamoxifen for prevention of breast cancer: report of the National Surgical Adjuvant Breast and Bowel Project P-1 Study. *J Natl Cancer Inst.* 1998;90(18):1371-88.
21. Burris HA, Hurwitz HI, Dees EC, Dowlati A, Blackwell KL, O'Neil B, et al. Phase I safety, pharmacokinetics, and clinical activity study of lapatinib (GW572016), a reversible dual inhibitor of epidermal growth factor receptor tyrosine kinases, in heavily pretreated patients with metastatic carcinomas. *J Clin Oncol.* 2005;23(23):5305-13.
22. Effects of chemotherapy and hormonal therapy for early breast cancer on recurrence and 15-year survival: an overview of the randomised trials. *Lancet.* 2005;365(9472):1687-717.
23. Tormey DC, Gray R, Falkson HC. Postchemotherapy adjuvant tamoxifen therapy beyond five years in patients with lymph node-positive breast cancer. Eastern Cooperative Oncology Group. *J Natl Cancer Inst.* 1996;88(24):1828-33.
24. Swain SM. Tamoxifen: the long and short of it. *J Natl Cancer Inst.* 1996;88(21):1510-2.
25. Chang J, Powles TJ, Allred DC, Ashley SE, Makris A, Gregory RK, et al. Prediction of clinical outcome from primary tamoxifen by expression of biologic markers in breast cancer patients. *Clin Cancer Res.* 2000;6(2):616-21.

26. Vogel CL, Cobleigh MA, Tripathy D, Gutheil JC, Harris LN, Fehrenbacher L, et al. Efficacy and safety of trastuzumab as a single agent in first-line treatment of HER2-overexpressing metastatic breast cancer. *Journal of Clinical Oncology*. 2002;20(3):719-26.
27. Jacobs MA, Ouwerkerk R, Wolff AC, Gabrielson E, Warzecha H, Jeter S, et al. Monitoring of neoadjuvant chemotherapy using multiparametric, (23)Na sodium MR, and multimodality (PET/CT/MRI) imaging in locally advanced breast cancer. *Breast Cancer Res Tr*. 2011;128(1):119-26.
28. Mankoff DA, Dunnwald LD, L. K., Doot RK, Specht JM, Gralow JR, Ellis GK, et al. PET Tumor Metabolism in Locally Advanced Breast Cancer Patients Undergoing Neoadjuvant Chemotherapy: Value of Static versus Kinetic Measures of Fluorodeoxyglucose Uptake. *Clinical Cancer Research*. 2011;17(8):2400-9.
29. Li SP, Makris A, Beresford MJ, Taylor NJ, Ah-See MLW, Stirling JJ, et al. Use of Dynamic Contrast-enhanced MR Imaging to Predict Survival in Patients with Primary Breast Cancer Undergoing Neoadjuvant Chemotherapy. *Radiology*. 2011;260(1):68-78.
30. Benard F, Aliaga A, Rousseau JA, Cadorette J, Croteau E, van Lier JE, et al. A small animal positron emission tomography study of the effect of chemotherapy and hormonal therapy on the uptake of 2-deoxy-2-[F-18]fluoro-D-glucose in murine models of breast cancer. *Mol Imaging Biol*. 2007;9(3):144-50.
31. Minami H, Kawada K, Murakami K, Sato T, Kojima Y, Ebi H, et al. Prospective study of positron emission tomography for evaluation of the activity of lapatinib, a dual inhibitor of the ErbB1 and ErbB2 tyrosine kinases, in patients with advanced tumors. *Jpn J Clin Oncol*. 2007;37(1):44-8.
32. Warburg O. On the origin of cancer cells. *Science*. 1956;123(3191):309-14.
33. Furman E, Rushkin E, Margalit R, Bendel P, Degani H. Tamoxifen induced changes in MCF7 human breast cancer: in vitro and in vivo studies using nuclear magnetic resonance spectroscopy and imaging. *J Steroid Biochem Mol Biol*. 1992;43(1-3):189-95.
34. Cheng CM, Cohen M, Wang J, Bondy CA. Estrogen augments glucose transporter and IGF1 expression in primate cerebral cortex. *FASEB J*. 2001;15(6):907-15.
35. Suarez E, Bach D, Cadefau J, Palacin M, Zorzano A, Guma A. A novel role of neuregulin in skeletal muscle. Neuregulin stimulates glucose uptake, glucose transporter translocation, and transporter expression in muscle cells. *J Biol Chem*. 2001;276(21):18257-64.
36. Zhang D, Tai LK, Wong LL, Chiu LL, Sethi SK, Koay ES. Proteomic study reveals that proteins involved in metabolic and detoxification pathways are highly

- expressed in HER-2/neu-positive breast cancer. *Mol Cell Proteomics*. 2005;4(11):1686-96.
37. Engelman JA, Luo J, Cantley LC. The evolution of phosphatidylinositol 3-kinases as regulators of growth and metabolism. *Nat Rev Genet*. 2006;7(8):606-19.
 38. Wang L, Zhang Q, Zhang J, Sun S, Guo H, Jia Z, et al. PI3K pathway activation results in low efficacy of both trastuzumab and lapatinib. *BMC Cancer*. 2011;11(1):248.
 39. Berns K, Horlings HM, Hennessy BT, Madiredjo M, Hijmans EM, Beelen K, et al. A functional genetic approach identifies the PI3K pathway as a major determinant of trastuzumab resistance in breast cancer. *Cancer Cell*. 2007;12(4):395-402.
 40. Cooper C, Liu GY, Niu YL, Santos S, Murphy LC, Watson PH. Intermittent hypoxia induces proteasome-dependent down-regulation of estrogen receptor alpha in human breast carcinoma. *Clin Cancer Res*. 2004;10(24):8720-7.
 41. Emptage NJ. Fluorescent imaging in living systems. *Curr Opin Pharmacol*. 2001;1(5):521-5.
 42. Chance B, Schoener B, Oshino R, Itshak F, Nakase Y. Oxidation-reduction ratio studies of mitochondria in freeze-trapped samples. NADH and flavoprotein fluorescence signals. *J Biol Chem*. 1979;254(11):4764-71.
 43. Drezek R, Brookner C, Pavlova I, Boiko I, Malpica A, Lotan R, et al. Autofluorescence microscopy of fresh cervical-tissue sections reveals alterations in tissue biochemistry with dysplasia. *Photochem Photobiol*. 2001;73(6):636-41.
 44. Gullledge CJ, Dewhirst MW. Tumor oxygenation: a matter of supply and demand. *Anticancer Res*. 1996;16(2):741-9.
 45. Kirkpatrick ND, Zou C, Brewer MA, Brands WR, Drezek RA, Utzinger U. Endogenous fluorescence spectroscopy of cell suspensions for chemopreventive drug monitoring. *Photochem Photobiol*. 2005;81(1):125-34.
 46. Mujat C, Greiner C, Baldwin A, Levitt JM, Tian F, Stucenski LA, et al. Endogenous optical biomarkers of normal and human papillomavirus immortalized epithelial cells. *Int J Cancer*. 2008;122(2):363-71.
 47. Skala MC, Riching KM, Gendron-Fitzpatrick A, Eickhoff J, Eliceiri KW, White JG, et al. In vivo multiphoton microscopy of NADH and FAD redox states, fluorescence lifetimes, and cellular morphology in precancerous epithelia. *P Natl Acad Sci USA*. 2007;104(49):19494-9.
 48. Ostrander JH, McMahon CM, Lem S, Millon SR, Brown JQ, Seewaldt VL, et al. Optical redox ratio differentiates breast cancer cell lines based on estrogen receptor status. *Cancer Res*. 2010;70(11):4759-66.

49. Huang S, Heikal AA, Webb WW. Two-photon fluorescence spectroscopy and microscopy of NAD(P)H and flavoprotein. *Biophys J*. 2002;82(5):2811-25. PMID: 1302068.
50. Piccart-Gebhart MJ, Procter M, Leyland-Jones B, Goldhirsch A, Untch M, Smith I, et al. Trastuzumab after adjuvant chemotherapy in HER2-positive breast cancer. *N Engl J Med*. 2005;353(16):1659-72.
51. Miller TW, Forbes JT, Shah C, Wyatt SK, Manning HC, Olivares MG, et al. Inhibition of mammalian target of rapamycin is required for optimal antitumor effect of HER2 inhibitors against HER2-overexpressing cancer cells. *Clin Cancer Res*. 2009;15(23):7266-76. PMID: 2787848.
52. Xia W, Bacus S, Hegde P, Husain I, Strum J, Liu L, et al. A model of acquired autoresistance to a potent ErbB2 tyrosine kinase inhibitor and a therapeutic strategy to prevent its onset in breast cancer. *Proc Natl Acad Sci U S A*. 2006;103(20):7795-800. PMID: 1472524.
53. Eng J, Lynch RM, Balaban RS. Nicotinamide adenine dinucleotide fluorescence spectroscopy and imaging of isolated cardiac myocytes. *Biophys J*. 1989;55(4):621-30. PMID: 1330544.
54. Ritter CA, Perez-Torres M, Rinehart C, Guix M, Dugger T, Engelman JA, et al. Human breast cancer cells selected for resistance to trastuzumab in vivo overexpress epidermal growth factor receptor and ErbB ligands and remain dependent on the ErbB receptor network. *Clin Cancer Res*. 2007;13(16):4909-19.
55. Rexer BN, Ham AJ, Rinehart C, Hill S, de Matos Granja-Ingram N, Gonzalez-Angulo AM, et al. Phosphoproteomic mass spectrometry profiling links Src family kinases to escape from HER2 tyrosine kinase inhibition. *Oncogene*. 2011;30(40):4163-74.
56. Griffith JB. Role of Serum, Insulin and Amino-Acid Concentration in Contact Inhibition of Growth of Human Cells in Culture. *Exp Cell Res*. 1972;75(1):47-&.
57. Specht JM, Kurland BF, Montgomery SK, Dunnwald LK, Doot RK, Gralow JR, et al. Tumor Metabolism and Blood Flow as Assessed by Positron Emission Tomography Varies by Tumor Subtype in Locally Advanced Breast Cancer. *Clinical Cancer Research*. 2010;16(10):2803-10.
58. Basu S, Chen W, Tchou J, Mavi A, Cermik T, Czerniecki B, et al. Comparison of triple-negative and estrogen receptor-positive/progesterone receptor-positive/HER2-negative breast carcinoma using quantitative fluorine-18 fluorodeoxyglucose/positron emission tomography imaging parameters: a potentially useful method for disease characterization. *Cancer*. 2008;112(5):995-1000.

59. Tan M, Zhao YH, Liu H, Liu ZX, Ding Y, LeDoux SP, et al. Overcoming Trastuzumab Resistance in Breast Cancer by Targeting Dysregulated Glucose Metabolism. *Cancer Research*. 2011;71(13):4585-97.
60. Smith TAD, Cheyne RW, Trembleau L, McLaughlin A. Changes in 2-fluoro-2-deoxy-D-glucose incorporation, hexokinase activity and lactate production by breast cancer cells responding to treatment with the anti-HER-2 antibody trastuzumab. *Nucl Med Biol*. 2011;38(3):339-46.
61. Reilly RM, McLarty K, Fasih A, Scollard DA, Done SJ, Vines DC, et al. (18)F-FDG Small-Animal PET/CT Differentiates Trastuzumab-Responsive from Unresponsive Human Breast Cancer Xenografts in Athymic Mice. *J Nucl Med*. 2009;50(11):1848-56.